# Backpropagation and decay of self-induced-transparency pulses

Robert Marskar* and Ulf L. Österberg†

*Department of Electronics and Telecommunication, Norwegian University of Science and Technology, N-7491 Trondheim, Norway*

(Received 31 May 2013; published 19 February 2014)

We demonstrate numerically that when the forward wave approximation of Maxwell's equations is not valid, the hyperbolic secant pulses of self-induced transparency gradually lose energy with increasing propagation distance through the excitation of a backward mode.

DOI: 10.1103/PhysRevA.89.023828 PACS number(s): 42.50.Gy, 42.50.Md, 42.65.Re

## I. INTRODUCTION

The nonlinear propagation of ultrashort light pulses tuned close to a resonance has led to the prediction and comprehension of a plethora of physical phenomena, such as adiabatic inversion [1], Rabi flopping [2], the spin echo [3], and self-induced transparency (SIT) [4], to name a few. In the nonresonant regime, the nonlinear Schrödinger equation, which is based on parametric wave amplification, stands out as a landmark, describing the complex interplay between linear and nonlinear wave effects. A feature common to the conventional description of all of these phenomena is that the laser pulse is assumed to propagate only in the forward direction and that it evolves slowly over an optical wavelength.

The pioneering work by McCall and Hahn [5], Lamb [6], Bullough and coworkers [7], and others has shown that optical self-induced transparency solitons of arbitrary duration and intensity can propagate close to an atomic resonance without losing energy provided that (i) the pulse duration $T$ is much shorter than the decoherence time $T_2$ of the material and (ii) backpropagation of the pulse can be ignored. The solitary pulse durations may be shorter or longer than the inhomogeneous lifetime $T_2^*$, although it was in the inhomogeneously broadened limit $T_2^* \ll T$ that the solitons were first discovered both theoretically and experimentally [5]. In this paper, we show that for materials where backpropagation cannot be neglected, these pulses naturally lose energy during propagation, which prevents the formation of an optical soliton over sufficiently long propagation distances.

## II. THEORETICAL MODEL

When a linearly polarized electromagnetic plane wave $\boldsymbol{E} = E_y(z)\hat{\boldsymbol{y}}$, $\boldsymbol{B} = B_x(z)\hat{\boldsymbol{x}}$ propagates in a two-level material, the Maxwell-Bloch model is summarized by Maxwell's curl equations and the von Neumann equation [8],

$$\dot{\Omega} = \Psi_\xi - \omega_\kappa \dot{p}, \quad \dot{\Psi} = \Omega_\xi, \tag{1a}$$

$$i\dot{\rho} = [H,\rho] + R, \quad H = \begin{pmatrix} 0 & -\Omega \\ -\Omega & \omega_s \end{pmatrix}, \tag{1b}$$

where the overdot indicates differentiation with respect to time and $\xi \equiv z/c$. The propagation axis is assumed to lie along $z$. In Eq. (1), the normalized electric and magnetic fields are $\Omega = \mu E_y/\hbar$ and $\Psi = \mu c B_x/\hbar$, where $\mu$ is the transition dipole moment (projected onto the $y$ axis) between the ground and excited states, $\rho = \rho(t,z;\omega_s)$ is the $2\times 2$ density matrix, and $R = R(\rho)$ is a relaxation superoperator. The resonance frequency of each isolated absorber is $\omega_s$, and the dielectric is inhomogeneously broadened with polarization $p$ and inversion $w$ given by $p = \int d\omega_s g(\omega_s)(\rho_{12} + \rho_{21})$ and $w = \int d\omega_s g(\omega_s)(\rho_{22} - \rho_{11})$, where $d\omega_s g(\omega_s)$ is the fraction of absorbers whose resonance frequencies lie on the interval $[\omega_s, \omega_s + d\omega_s]$. The coupling frequency $\omega_\kappa$ is defined $\omega_\kappa = \mathcal{N}\mu^2/\hbar\epsilon_0$, where $\mathcal{N}$ is the number density of the material. Introducing the pseudofields $\Omega^\pm = \frac{1}{2}(\Omega \mp \Psi)$, the normalized Poynting vector can be written $\boldsymbol{S} = -\Omega\Psi\hat{\boldsymbol{z}} = \Omega^{+2} - \Omega^{-2}$. $\Omega^\pm$ represent the forward- and backward-propagating fields, and a scaling argument can be used to show that $\Omega^-$ is negligible when $\Omega$ initially propagates in the forward $(+\xi)$ direction and $\Omega \gg \omega_\kappa p$ [7]. This condition is equivalent to slow spatial evolution over an optical wavelength, and Eq. (1a) then reduces to $\dot{\Omega} + \Omega_\xi = -\frac{\omega_\kappa}{2}\dot{p}$. This equation is a first -order wave equation along the forward characteristic $t = \xi$; it is valid for arbitrary pulse durations and can, together with Eq. (1b), be solved with the inverse scattering transform technique [7]. The equation has both soliton and breather solutions, with the latter solution being mathematically equivalent to the McCall-Hahn $2\pi$ soliton in the case of long pulses. However, $\omega_\kappa$ can become quite large in, e.g., high-pressure alkali-metal vapors, organic dyes, or doped semiconductors. Backpropagation is then possible *a priori*, and a relatively large reflective loss from the vacuum-material interface must also be accepted. Note that the two-level model is only phenomenological for semiconductors, insofar that the quasicontinuous bands of semiconductors can only behave like a single inhomogeneously broadened resonance if the intraband decoherence times are much shorter than the pulse duration. There is also a correspondence between the Maxwell-Bloch equations and the theory of large-area Josephson junctions [9]. Note that when $\Omega \sim \omega_\kappa p$ local-field effects may become noticeable [10]. The effect that we discuss here, however, is primarily concerned with the breakdown of the forward wave approximation of Maxwell's equations, and for comparison with known theoretical results, we have provisionally ignored local-field effects and retained the macroscopic field $\Omega$ in the Hamiltonian in Eq. (1b).

In this paper, we solve Eq. (1) numerically for up to 5000 values of $\omega_s$ by using a hybrid Message Passing Interface (MPI) and Open Multi-Processing (OpenMP) pseudospectral operator-splitting method that is discussed elsewhere in detail [11]. We consider a Gaussian input pulse $\Omega(t,0) = \Omega_0 \exp[-t^2/(2T^2)]\sin(\omega_c t)$ that is emitting from

*robert.marskar@iet.ntnu.no
†ulf.osterberg@iet.ntnu.no

 

a total-field–scattered-field [12] source at $z = 0$ in vacuum. This pulse propagates in free space for 250 $\mu$m before it penetrates a two-level material of length $L$ and then exits back into free space again. We do not make envelope or rotating-wave approximations, and $\{\Omega, \Psi\}$ denotes the full electromagnetic field. Our simulation region is padded with perfectly matched layers that prevent back reflection from the truncated simulation region.

In what follows, the center of the absorption line is placed at $\overline{\omega}_s = 6\pi \times 10^{13}$rad/s ($\overline{\lambda} = 10\mu$m), $\mu = 5$D, $g(\omega_s) = (T_2^*/\sqrt{2\pi})\exp[-(\omega_s - \overline{\omega}_s)^2 T_2^{*2}/2]$, and $T_2^* = 50$ fs. Homogeneous damping, which removes the energy that is locked in the dipoles via, e.g., spontaneous emission or through other channels, is accounted for via $R$, with $T_1 = 1$ms and $T_2 = 0.1$ms, substantially longer than the pulse duration. The spatial and temporal discretization lengths are $\triangle z = \overline{\lambda}/100$ and $\triangle t = 2\triangle z/(\pi c)$, and we have verified that the output from our computer simulations does not change with increased resolution. In the following, we consider a resonant Gaussian input pulse ($\omega_c = \overline{\omega}_s$) with peak amplitude $E_0 = 8.27 \times 10^7$V/m ($\Omega_0 \approx 10^{13}$rad/s) and duration $T = 250$ fs. This fixes the input area defined by the Gaussian envelope slightly below $2.6\pi$ and ensures that the input pulse is a temporally slowly varying pulse $\omega_c T \sim 50$. We are therefore in the conventional SIT regime where the pulse duration fits between the two transverse lifetimes ($T_2 \gg T > T_2^*$). Note that as an alternative to solving Eq. (1) directly, separate inhomogeneous evolution equations for $\Omega^{\pm}$ that are coupled through Eq. (1b) are easily derived from Eq. (1a) and can also be solved numerically.

## III. TRADITIONAL SIT REGIME

First, we verify that the standard SIT behavior is recovered in the limit $\omega_\kappa \ll \Omega_0$. We take $\mathcal{N} = 5 \times 10^{23}$m$^{-3}$ and $L = 2.5$ mm, which gives $\Omega_0 \approx 88\omega_\kappa$. The optical density of the dielectric is $\alpha L \approx 14.5$, where $\alpha = \pi\omega_\kappa \overline{\omega}_s g(\overline{\omega}_s)/c$ is the reciprocal absorption length [8]. With the numbers above, $\alpha^{-1} \approx 17.2\overline{\lambda} = 172\,\mu$m. Figure 1 shows that the standard SIT features, which are expected to hold at these conditions, are captured by our numerical code: The initial pulse partially reflects while the remaining energy penetrates the material. It is then compressed and amplified over the first few absorption lengths and reshapes into a hyperbolic secant pulse with pulse area $2\pi$ which propagates stably and with constant energy. We have calculated the pulse area as the Fourier transform of $\Omega(t,z)$ on the line center, i.e., $\theta(z) = |\Omega(\overline{\omega}_s, z)| = |\int_{-\infty}^{\infty} \Omega(t,z)e^{-i\overline{\omega}_s t}dt|$, and the pulse energy is found by integration of the Poynting vector. The top panel in Fig. 1 shows that the computer solution agrees very well with the area theorem $\theta(z) = 2n\pi + \arctan[\exp(-\alpha z/2)\tan(\theta_0/2)]$, where $\theta_0$ is the input area. We nevertheless point out that it is the soliton feature and not the area theorem which is the fundamental property of the system. Although the soliton feature holds whenever $T \ll T_2$ and backpropagation can be ignored (even when the slowly varying and rotating-wave approximations are not valid), the area theorem holds only when the initial pulse is resonant, transform limited, and slowly varying through the material and the absorption line is symmetric around $\overline{\omega}_s$ [13]. These conditions are fulfilled by the parameters above. The bottom panel in Fig. 1 shows

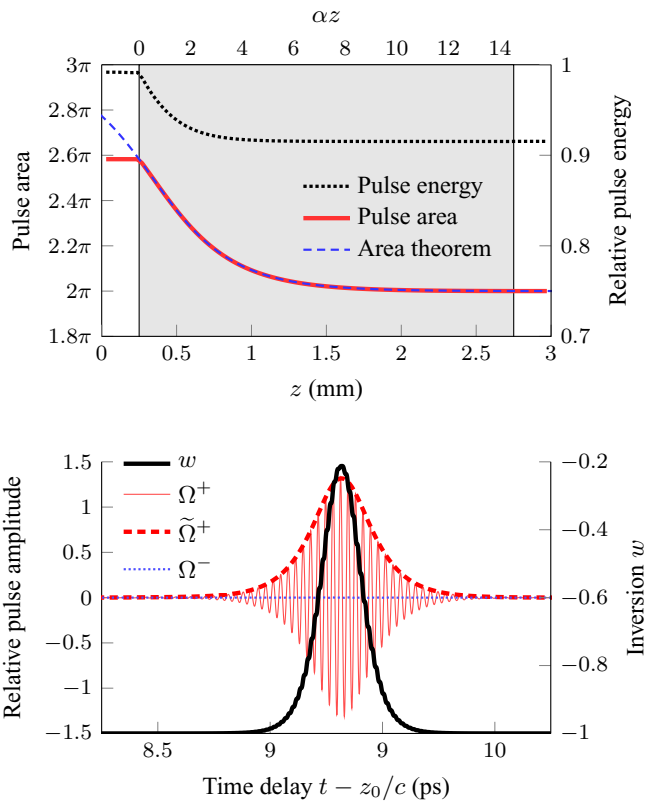


FIG. 1. (Color online) (top) Normalized pulse energy (dotted line, plotted against the right vertical axis) and area (solid line) compared with the area theorem (dashed line). (bottom) Average material inversion $w$ (thick solid line, plotted against the right vertical axis). Plotted against the left vertical axis is the forward field $\Omega^+$ (thin solid line), its envelope (dashed line), and the backward field $\Omega^-$ (dotted line). The data are taken from a distance $z_0 = 1.75$ mm ($\alpha z_0 \approx 10$) into the material.

the auxiliary fields $\Omega^{\pm}$ and their corresponding envelopes $\widetilde{\Omega}^{\pm}$ after penetrating 2 mm into the dielectric. We have obtained the envelopes $\widetilde{\Omega}^{\pm}$ via the analytic signals of $\Omega^{\pm}$. The full electric-field profile coincides with the forward field $\Omega^+$ and has been confirmed to be a hyperbolic secant with area $\approx 2\pi$. It inverts the material and completely reverts it to its ground state. The presence of the negative flux field $\Omega^-$ is clearly negligible. After the formation of the $2\pi$ pulse, the long-time behavior of the system is $\Omega^{\pm}(t \to \infty, z) = 0$ and $w(t \to \infty, z) = -1$, which makes this particular pulse a SIT pulse.

## IV. BACKPROPAGATION AND DECAY OF SIT PULSES

Having established the reliability for our model with $\Omega \gg \omega_\kappa p$, we can now address the main reason for this paper, namely, the regime $\Omega \sim \omega_\kappa p$, where backpropagation has a non-negligible effect. The density is taken as $\mathcal{N} = 4.4 \times 10^{25}$m$^{-3}$, which gives $\Omega_0 \approx \omega_\kappa$. The absorption length is $\alpha^{-1} \approx 0.195\overline{\lambda}_s$, and the material is essentially opaque for linear transmission of resonant radiation. We take the length of the material to be $L = 0.5$ mm long so that its optical thickness is $\alpha L \approx 256$. We consider the same Gaussian input pulse. The top panel in Fig. 2 shows the envelopes $\widetilde{\Omega}^+$ and $\widetilde{\Omega}^-$ a distance

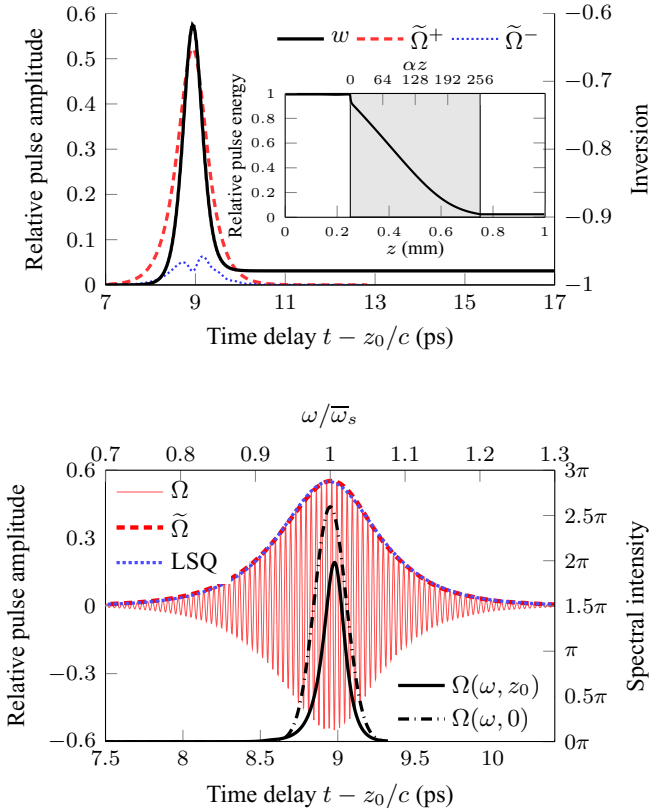


FIG. 2. (Color online) (top) Plotted against the left vertical axis are the envelopes of $\Omega^+$ (dashed line) and $\Omega^-$ (dotted line). The inversion $w$ (solid line) is plotted against the right vertical axis. The inset shows the pulse energy normalized to the input pulse energy as a function of propagation distance. (bottom) Full field $\Omega$ (thin solid line) and its envelope (dashed line) compared with an LSQ fit of a hyperbolic secant pulse (dotted line). Plotted against the second set of axes is the input pulse spectrum (dashed-dotted line) and the spectrum $\Omega(\omega,z_0)$ (thick solid line). The data in both panels are taken at a propagation length of $z_0 = 0.25$ mm ($\alpha z_0 \approx 128$) into the material.

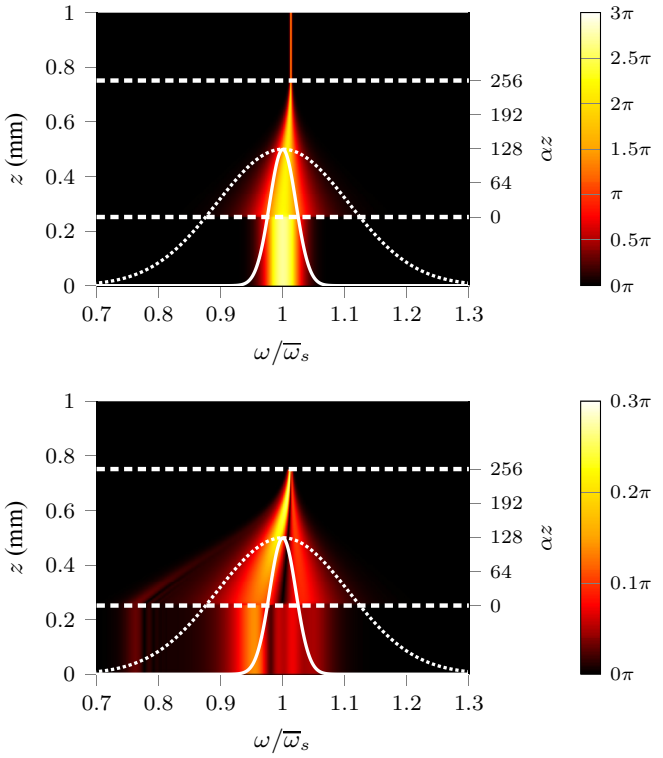


FIG. 3. (Color online) (top) Spatial propagation of the spectrum of $\Omega^+$ (color coded) inside and outside the material, the inhomogeneous absorption line $g(\omega_s)$ (dotted line), and the initial pulse spectrum $\Omega(\omega,0)$ (solid line). The dashed lines show the material-vacuum interface. (bottom) Same as for the top panel, but for $\Omega^-$.

$z_0 = 0.25$ mm into the material, and the negative flux field $\Omega^-$ is readily discerned. The most important difference between the behaviors in Figs. 1 and 2 lies in the fact that $\Omega^+ \neq \Omega$ and that the long-term behavior is $w(t \to \infty, z) \neq -1$ for the denser material. In Fig. 2 we see that $\Omega^{\pm}(t \to \infty) = 0$, $w(t \to \infty) \approx -0.98$, and the pulse leaves behind energy in the material. It is therefore not an SIT soliton. This failure to return the material to the ground state after the passage of the pulse is not related to the initial shedding of energy that usually takes place when a non-SIT pulse reshapes into a soliton under ideal SIT conditions, which is seen in Fig. 1 as an initial decline in pulse energy over the first absorption lengths. Even at a distance $z_0 = 0.25$ mm into the material, the pulse in Fig. 2 has propagated $\alpha z_0 \approx 128$ absorption lengths, a substantial distance. Under ideal SIT conditions (i.e., no backpropagation or other losses), a $2\pi$ soliton would be expected at this penetration depth. Here, the pulse instead leaves behind a trail of inversion $w > -1$, and a soliton does not form. The inset in the top panel in Fig. 2 shows that although the residual material excitation is relatively small, it has a profound impact on the pulse over many absorption lengths. The initial dip in energy is associated with the initial reshaping into a sech pulse, while the decay from $\alpha z \approx 10$ to $\alpha z \approx 256$ is connected to a backpropagation loss. It is interesting that this decay is almost linear up to $\alpha z \approx 170$ and that the final state of inversion lies close to $-1$, which is indicative of a small-area backward-propagating pulse. Indeed, as seen in the top panel of Fig. 2, the area under $\widetilde{\Omega}^+$ is much larger than that under $\widetilde{\Omega}^-$. The flattening of the pulse energy after $\alpha z \sim 170$ is most likely due to an edge effect where the backpropagating pulse is being generated from a smaller spatial region. To expose the pulse in greater detail, the bottom panel in Fig. 2 shows the full field $\Omega$ and a comparison between the corresponding envelope $\widetilde{\Omega}$ (dashed line) and a numerical least squares fit (LSQ, dotted line) of a hyperbolic secant pulse envelope $f(t) = A \operatorname{sech}[(t - t_0)/\tau]$. The pulse in Fig. 2, unlike the pulse in Fig. 1, is not a pure $2\pi$ hyperbolic secant pulse, although it remains so to a very good approximation. Plotted against the right vertical axis in Fig. 2(b) is also the spectral intensity of the pulse. We notice that the center frequency of the pulse is slightly blueshifted to a value of $\approx 1.005\overline{\omega}_s$.

To compare the forward and backward fields, the two panels in Fig. 3 show the propagated spectra of $\Omega^{\pm}$ plotted together with the inhomogeneous broadening line $g(\omega_s)$ (dotted line) and also the initial pulse spectrum $\Omega(\omega,0)$ (solid line). Several features of the computer solution deserve mention: First, we observe that the forward spectrum broadens over the first few Beer's lengths, indicating that temporal compression of the

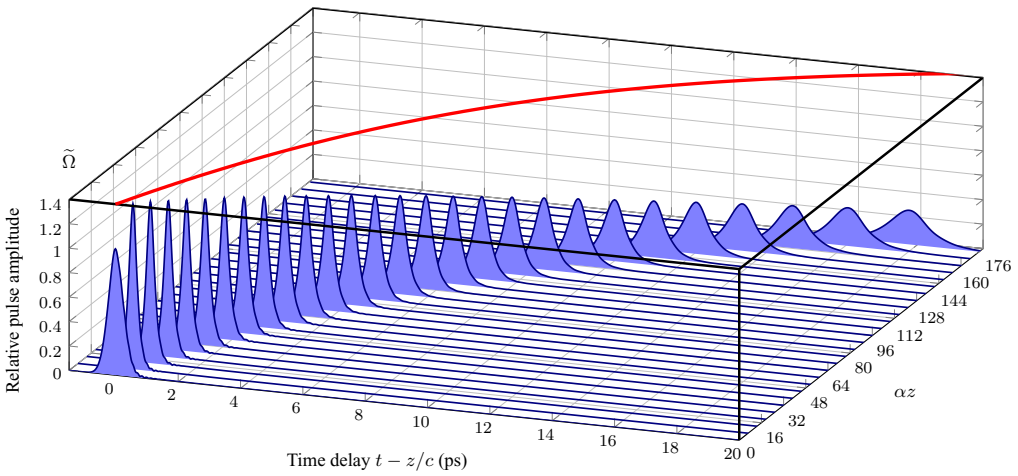


FIG. 4. (Color online) Spatiotemporal reshaping over the first 176 absorption lengths. The two horizontal axes are the pulse delay $t - z/c$ and the propagation distance in units of $\alpha^{-}$. The vertical axis indicates the magnitude of the full field pulse envelope. The solid line plotted in the top horizontal plane shows the peak time delay at the various propagation distances.

pulse due to spatiotemporal reshaping into a quasi-SIT pulse is taking place. The subsequent narrowing of the spectrum is due to backpropagation losses that lead to temporal elongation. Note also that although the spectral intensity of the input pulse around $\omega/\overline{\omega}_s \approx 0.78$ is zero, there is such a peak in the spectrum of the reflected field $\Omega^{-}$ and no such feature for $\Omega^{+}$. Nonlinear reflection from interfaces has been studied by others [14] in the incoherent regime $T_2 \ll T \ll T_1, T_2^*$, and a redshift has been predicted due to the Doppler-shifted reflection from the moving saturation front that is formed in the material when the pulse penetrates the interface. This explanation presumably holds true here as well. The pulse velocity $v$ near the interface in Fig. 4 is roughly $v/c \approx 0.11$ and matches the Doppler shift $\Delta\omega \approx 0.22\overline{\omega}_s$. The small color shifts of $\Omega^{\pm}(\omega,z)$ during propagation are, to the best of our knowledge, not predicted by any existing theory. It is established, on the other hand, that if the rotating-wave and slowly varying envelope approximations in time and space are valid, Eq. (1) can be reduced to a set of equations relating only to the pulse envelope for the forward-propagating pulse and that frequency pushing of an initially off-resonance $2\pi$ hyperbolic secant soliton may then occur [15]. In our computer simulations, the input pulse is resonant and transform limited; therefore any initial pulse chirp or change in center frequency occurs as a result of either bi-directional propagation, or frequency-biased reflection or transmission from the interface.

Figure 4 shows the spatiotemporal reshaping that is induced by the backward-propagating mode. The two horizontal axes are the temporal pulse delay $t - z/c$ and the propagation distance $z$ into the medium in units of $\alpha^{-1}$. Only the spatiotemporal reshaping over the first 176 absorption lengths is shown. The solid line plotted in the top plane indicates the peak pulse delay at various $z$. Its curvature in the $(t - z/c, z)$ plane indicates a nonconstant group velocity. We find that over the first few absorption lengths the pulse is temporally compressed. This initial reshaping is not surprising considering the initial conditions that are applied. According to the area theorem, which holds as a first approximation over the first absorption lengths, the Fourier coefficient of $\Omega^{+}(\overline{\omega}_s, z)$ must decrease to $2\pi$ during the initial reshaping to a hyperbolic secant pulse. During this reshaping the excess spectral energy at the line center is either absorbed by the medium or pushed into the spectral wings of the pulse, which results in spectral broadening and temporal compression. With further propagation we observe the nonstandard features: As the pulse energy diminishes with increasing propagation distance, the temporal pulse width increases, and the pulse travels with further reduced group velocity. For an even longer material, the pulse will eventually broaden to time scales that are comparable to the homogeneous decoherence time $T_2$ and is then rapidly absorbed by the material. This type of pulse stretching is typical of solitonic systems with loss and has been studied by others through the introduction of phenomenological loss terms in the envelope forms of Eq. (1) (see, e.g., [15, 16]). The loss mechanism considered here is not phenomenological but is an inevitable part of Maxwell's wave equation. It will be finite also for less dense materials having the same optical thickness, although homogeneous damping will then dominate. To our knowledge, the only soliton solution to Eq. (1) known at present is the half-cycle hyperbolic secant $\Omega(t,z) = \Omega_0 \operatorname{sech}[\Omega_0(t - mzc^{-1})]$ (i.e., a hyperbolic secant without carrier) [17] and its $N$-soliton generalizations. These solitary pulses do not satisfy the multidimensional Maxwell's equations in vacuum and are presently therefore of little practical relevance. Whether such solitons can stabilize in a material through a compensation of self-focusing and diffractive effects is an intriguing question and requires a study of the three-dimensional Maxwell-Bloch equations. To the best of our knowledge, such a study has not been performed to date.

We now briefly mention that if the inhomogeneous lifetime becomes longer such that $T < T_2^* \ll T_1, T_2$, the pulse behavior changes, and a larger blueshift (see, e.g., [18] for the sharp-line case) can move the pulse completely outside the absorption band of the material where it can propagate a longer distance. Nevertheless, we have numerically verified also for dense media that off-resonant hyperbolic secant pulses are also incapable of completely returning the material back to the ground state and also lose energy during propagation, although

to a considerably smaller extent than for resonant pulses in inhomogeneously broadened media. Obviously, in the artificial undamped limit $T_1, T_2, T_2^* \to \infty$ the excited dipoles radiate forever, and optical transparency is difficult to avoid. Additionally, insofar as SIT is valid down to the single cycle regime, so are the results of this paper. The generalization of the $2\pi$ McCall-Hahn soliton for arbitrary durations is the $2\pi$ breather solution

$$\Omega(t,z) = 2\Omega_0 \operatorname{sech}\theta_R \frac{\cos\theta_I - \gamma \sin\theta_I \tanh\theta_R}{1+\gamma^2 \sin^2\theta_I \operatorname{sech}^2\theta_R}, \qquad (2)$$

where $\theta_R = \frac{1}{2}\Omega_0(t - m_e z/c) + \delta_R$, $\theta_I = \omega_c(t - m_c z/c) + \delta_I$ and $\gamma = \Omega_0/(2\omega_c)$. Equation (2) is valid in the forward wave approximation $\Omega \gg \omega_\kappa p$. The expressions for the refractive indices $m_e$ and $m_c$ in the sharp-line regime are found in, e.g., [7]. We have verified that the breather solution Eq. (2) coincides with our computer solution when we consider close-to single-cycle input pulses and that when the forward wave approximation is not valid, these pulses also leave the material slightly excited after they have passed.

The energy vs distance decay of SIT pulses has a complicated structure that depends on the input pulse shape and the relation between the pulse duration and the transverse and longitudinal lifetimes. For example, after exciting the medium with non-SIT pulses of duration $T < T_2^*$ in the unidirectional approximation, a long-lived precursor might precede the driving pulse [11]. Even when the soliton has formed after many Beer's lengths, this forerunner might persist due to its spectral location around the wings of the absorption line, where it experiences little absorption. In the case of a SIT pulse propagating in an inhomogeneously broadened attenuator, which is the scenario considered in this paper, the energy decay is adequately explained by phenomenologically incorporated loss terms in the Bloch equations. Figure 5 shows a computer solution of the propagation of the pulse above, but under the rotating-wave and slowly varying envelope approximations and with the inclusion of a spontaneous emission lifetime $T_1 = 20$ ps. That is, this pulse fits between the two transverse lifetimes $T_2^* < T < T_2$. Although the long-term behavior of this system is $w \to -1$, the same qualitative pulse behavior is recovered in this simplified model. The pulse energy decays linearly with propagation distance; the pulse broadens temporally and propagates with a reduced group velocity. On the whole, the propagational results of this paper may therefore be understood in terms of unidirectional solitonic SIT systems with phenomenologically incorporated loss terms.

This work also relates to recent studies of the area theorem using Eq. (1) in the undamped limit: Hughes [19] considered propagation of initial pulses $\Omega(t,0) = \Omega_0 \operatorname{sech}[t/T]\sin(\omega_c t)$

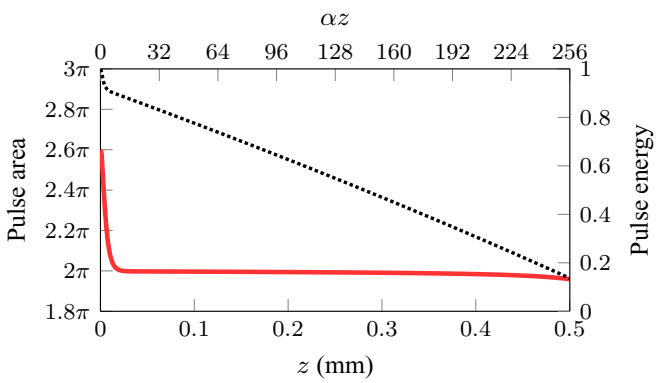


FIG. 5. (Color online) Energy vs distance (dotted line) and area vs distance (solid line) for a computer solution under the rotating-wave and slowly varying envelope approximations. The conditions are the same as in Figs. 2–4, but neglecting backpropagation and including a spontaneous emission lifetime of 20 ps.

with areas between $2\pi$ and $12\pi$ [i.e., $\Omega_0/(2\omega_c) \sim 0.1 - 1$] and showed that these pulses did not return the material to its initial state. A similar analysis was done by Xiao [20] and Novitsky [21]. We remark that if the Rabi frequency is comparable to $\omega_c$, then in view of Eq. (2) the initial pulses used in [19–21] are not SIT pulses but must be reshaped by the material before propagating as solitons. The residual energy left behind in the material in [19,21] is a sign of this reshaping. With the indicated parameters in Refs. [19–21] these systems are nevertheless solitonic, supporting SIT pulses down to arbitrary durations.

## V. CONCLUSIONS

In summary, by integrating the Maxwell-Bloch equations numerically, we show that backpropagation is relevant for self-induced transparency pulses in dense inhomogeneously broadened materials. The backward-propagating pulse is coexcited along with the forward-propagating pulse. After the pulse has passed, the atoms are left in an excited state. In this way, the pulse gradually loses energy; it elongates temporally and travels with reduced group velocity. A large redshift in the reflected radiation is predicted. Essential SIT results are reproduced for weaker materials where backpropagation is negligible.

## ACKNOWLEDGMENTS

This research was partially supported by the Norwegian University of Science and Technology with computational resources provided by NOTUR.

[1] D. Grischkowsky, Phys. Rev. Lett. **24**, 866 (1970); D. Grischkowsky and J. A. Armstrong, Phys. Rev. A **6**, 1566 (1972); D. Grischkowsky, E. Courtens, and J. A. Armstrong, Phys. Rev. Lett. **31**, 422 (1973).

[2] I. I. Rabi, Phys. Rev. **51**, 652 (1937).

[3] E. L. Hahn, Phys. Rev. **80**, 580 (1950).

[4] C. K. N. Patel and R. E. Slusher, Phys. Rev. Lett. **19**, 1019 (1967); H. M. Gibbs and R. E. Slusher, *ibid.* **24**, 638 (1970); Phys. Rev. A **6**, 2326 (1972); R. E. Slusher and H. M. Gibbs, *ibid.* **5**, 1634 (1972).

[5] S. L. McCall and E. L. Hahn, Phys. Rev. Lett. **18**, 908 (1967); Phys. Rev. **183**, 457 (1969).

[6] G. L. Lamb, Rev. Mod. Phys. **43**, 99 (1971).
[7] R. K. Bullough, P. J. Caudrey, J. C. Eilbeck, and J. D. Gibbon, Opt. Quantum Electron. **6**, 121 (1974); R. K. Bullough, P. M. Jack, P. W. Kitchenside, and R. Saunders, Phys. Scr. **20**, 364 (1979); J. C. Eilbeck, J. D. Gibbon, P. J. Caudrey, and R. K. Bullough, J. Phys. A **6**, 1337 (1973).
[8] L. Allen and J. H. Eberly, *Optical Resonance and Two-Level Atoms*, 2nd ed. (Dover, New York, 1987).
[9] R. K. Bullough, J. Mod. Opt. **47**, 2029 (2000).
[10] J. J. Maki, M. S. Malcuit, J. E. Sipe, and R. W. Boyd, Phys. Rev. Lett. **67**, 972 (1991).
[11] R. Marskar and U. Österberg, Opt. Express **19**, 16784 (2011).
[12] A. Taflove and S. C. Hagness, *Computational Electrodynamics: The Finite Difference Time-Domain Method*, 3rd ed. (Artech House, Boston, 2005).
[13] D. J. Kaup, Phys. Rev. A **16**, 704 (1977).
[14] W. Forysiak, R. G. Flesch, J. V. Moloney, and E. M. Wright, Phys. Rev. Lett. **76**, 3695 (1996).
[15] G. L. Lamb, Phys. Rev. Lett. **31**, 196 (1973); R. T. Deck and G. L. Lamb, Phys. Rev. A **12**, 1503 (1975); J. C. Diels and E. L. Hahn, *ibid*. **8**, 1084 (1973).
[16] A. M. Alhasan, J. Fiutak, and W. Miklaszewski, Z. Phys. B **88**, 349 (1992).
[17] R. K. Bullough and F. Ahmad, Phys. Rev. Lett. **27**, 330 (1971).
[18] V. P. Kalosha and J. Herrmann, Phys. Rev. Lett. **83**, 544 (1999).
[19] S. Hughes, Phys. Rev. Lett. **81**, 3363 (1998).
[20] J. Xiao, Z. Wang, and Z. Xu, Phys. Rev. A **65**, 031402 (2002).
[21] D. V. Novitsky, Phys. Rev. A **86**, 063835 (2012).